PAPER

Check for updates

Heterogeneous ion exchange membranes based on thermoplastic polyurethane (TPU): effect of PSS/DVB resin on morphology and electrodialysis

Muhammad Ahmad, [ID] Asif Ali Qaiser, [ID]* Noor Ul Huda [ID] and Anem Saeed

In this research, novel heterogeneous cation exchange membranes based on thermoplastic polyurethane (TPU) have been prepared by the solution casting technique. The effects of incorporation level of sulfonated polystyrene divinyl-benzene (PSS/DVB) resin on water uptake, ion exchange capacity, membrane potential and salt extraction have been elucidated. Morphological and water uptake studies suggested a two-phase heterogeneous membrane morphology owing to the presence of hard and soft segments in the TPU backbone and swelling of PSS/DVB particles. This morphology was shifted to a semi-gelled morphology throughout the membrane bulk when resin loading exceeded 50 wt%. The physically cross-linked hard segments in the TPU backbone ensured a compact membrane morphology and prevented the formation of water channels. The membrane potential showed that increasing the resin content increased the membrane transport number (max. 0.95) up to 50 wt% resin loading and beyond this, the transport number started decreasing showing a pronounced effect of voids and water flow channels developing on excessive swelling. The permselectivity reached a maximum (up to 0.92) and salt extraction values also increased (by varying voltage) up to 50 wt% loading and started decreasing beyond this optimum content. This study shows successful development of low-cost heterogeneous cation exchange membranes based on TPU with acceptable electrochemical properties.

1. Introduction

Membrane separation is a relatively emerging separation technology that has already found widespread applications on both industrial and domestic scale. A variety of membranes have been developed by varying microstructure and/or functionality for processes such as microfiltration, ultrafiltration, reverse osmosis, pervaporation and electrodialysis (ED). The electrodialysis process using ion exchange membranes (IEMs) is a highly selective process that is used in desalination of brackish/saline water, cheese whey demineralization, sodium chloride production and fuel cell technology.[1,2] The performance of an ion exchange membrane strongly depends on the degree of swelling, ion exchange capacity (IEC), dimensional stability, and chemical, oxidation and electrical resistances.[3–5] Ion exchange membranes are categorized as homogeneous or heterogeneous membranes based on the distribution of ion exchange moieties in a continuous membrane matrix. The heterogeneous membranes have good mechanical properties but lower electrochemical performance whereas the homogeneous membranes show excellent electrochemical properties with lower mechanical characteristics.[6,7] The performance of

a low-cost heterogeneous ion exchange membrane can be optimized by varying its composition (*i.e.* ion exchange resin, binder and additives) and physical parameters (*i.e.*, thickness, porosity *etc.*). The heterogeneous ion exchange membranes are synthesized by incorporating ion exchange resin particles in a polymer binder using various techniques such as calendaring an ion exchange resin into a polymer film, compression molding an inert polymer film with ion exchange resin particles and by solution casting technique.[6] The research in last few decades focused on producing high performance ion exchange membranes with low-cost and improved properties. This improvement also involved various modifications to existing membrane systems such as additive incorporation, membrane surface modification, solvent effects, ion exchange resin pre-treatment and membrane post-treatment *etc.* A few thermoplastic polymers have been used as membrane matrix in heterogeneous ion exchange membranes. Hosseini *et al.*[8] modified polyvinyl chloride (PVC) based heterogeneous ion exchange membranes with silver particles coating these at the surface using thermal plasma treatment. The effect of temperature on electrochemical characteristics was studied where increasing transport number was reported with modification extent. Malik *et al.*[5] fabricated PVC based heterogeneous cation exchange membranes and studied the effects of *in situ* polyaniline (PANI) deposition on the electrochemical properties by employing different polymerization techniques. Ariono *et al.*[9]

Department of Polymer and Process Engineering, University of Engineering and Technology, Lahore 54890, Pakistan. E-mail: asifaliqaiser@uet.edu.pk; Tel: +92 306 3798 108

studied polysulfone/polyethylene glycol (PEG) blend heterogenous cation exchange membranes with varying composition of PEG and resin particles. The concentration of PEG in membrane increased ion exchange capacity and water uptake. Vyas et al.[10] synthesized PVC based heterogeneous ion exchange membranes and reported the effects of resin content and particle size on ion exchange capacity and transport number. Moghadassi et al.[11] incorporated multiwalled carbon nanotubes (MWCNT) and used in situ polymerization of acrylic acid for surface modification of heterogeneous ion exchange membranes to improve ion exchange capacity and membrane conductivity. Hosseini et al.[12] fabricated polyacrylic acid copolymer polymethyl methacrylate/PVC (PAA-co-PMMA/PVC) based heterogeneous cation exchange membranes using graft polymerization technique. Increasing the ratio of emulsifier to monomers improved ion exchange capacity and electrochemical properties of these composite membranes. In recent studies on thermoplastic ion exchange membranes, the effects of incorporating magnetic nanoparticles (CoFe$_2$O$_4$) and bis(8-hydroxyquinoline)zinc (ZnQ$_2$) nanoparticles in PVC matrix on membranes morphology, swelling, transport number and permselectivity were reported.[3,4]

Thermoplastic polyurethane (TPU) is an engineering thermoplastic that has high flexibility and good impact, abrasion and environmental resistance, and shows good mechanical properties.[13] The chain structure of TPU is composed of soft and hard segments that imparts properties of both rubber-like and amorphous thermoplastics to TPU.[14,15] The soft segment is either polyether or polyester (polyester in the present study) with molecular weight ranging from 1000–3000 and the hard segments are diisocyanate functionalities reacted with a diol.[16] The hard segments in TPU form physical cross-links by strong hydrogen bonding between urethane–urethane and urethane–ester groups across the chains (Fig. 1).[16] The combination of hard and soft segments influences the mechanical properties of the membranes along with affecting permeation rate and selectivity in gas separation, desalination and pervaporation membranes.[17–22] The interaction of these hard and soft segments with the permeating species at molecular level controls the rate and selectivity of the separation processes. Moreover, the fouling resistance of TPU increases because of its tuneable hydrophilicity that is an advantage in membrane technology.[23] Only a very limited number of studies have been conducted using TPU as a matrix in ion exchange membrane applications.[24,25] Amado et al.[25] used TPU membrane matrix for heterogeneous cation exchange membranes by incorporating electroconductive polyaniline as filler. This originates the need of a systematic exploration of the effects of various membranes parameters on TPU based ion exchange membranes particularly the effect of cation exchange resin content on membrane structure, ion exchangeability and electrochemical properties.

Polyester based partially hydrophilic TPU has been used as membrane matrix in this research. This study shows a unique TPU membrane morphology based on the combination of hard and soft segments of TPU in conjunction with high degree of swellability of cation exchange resin embedded in the matrix. As a result, a novel membrane system has emerged where the swellability and membrane morphology depended on the TPU backbone chain structure and ion exchange resin loading, as well. The shifting of membrane morphology from a compact heterogeneous membrane to a highly swollen semi-gelled phase is related to ion exchange resin content and the effects of this semi-gelled morphology on membrane's properties and electrochemical performance have been elucidated in terms of transport numbers, perm-selectivity and salt extraction in electrodialysis.

2. Materials and methods

2.1 Materials

Commercial grade cation exchange resin (PSS/DVB, sulfonated polystyrene cross-linked divinyl benzene, Purolite® C100E) was purchased from local market and used after grinding to −400 mesh size. Polyester based thermoplastic polyurethane (TPU) (68T series, Bangtail Polymeric New Materials Corp. Korea) was purchased from local market. Commercial heterogeneous anion exchange membrane (AMI-7001, ion exchange capacity, IEC = 1.3 meq. g^{-1}) was supplied by Membrane International Inc. Methyl ethyl ketone (MEK) (Daejung, Korea), hydrochloric acid (Daejung, Korea), sodium chloride (Sigma-Aldrich), sodium hydroxide (Sigma-Aldrich), phenolphthalein (Merck) were all reagent grade and used as received. In all experiments, distilled water was used to prepare various solutions.

2.2 Pre-treatment of ion exchange resin

Sulfonated polystyrene divinyl benzene (PSS/DVB) cation exchange resin (ion exchange capacity = 2.0 meq. g^{-1}) was crushed in a rod mill and soaked in distilled water for 24 h. Subsequently, it was further ground using pestle and mortar, dried at 40 °C for 6 h and passed through a 400 mesh screen.

2.3 TPU-PSS/DVB membranes preparation

Heterogeneous cation exchange membranes were prepared by solution casting and subsequent solvent evaporation technique. Thermoplastic polyurethane (TPU) was dissolved in methyl ethyl ketone (2 : 8 w/v% of TPU-PSS/DVB and methyl ethyl ketone, respectively) at room temperature. The solution was kept under continuous stirring using magnetic stirrer for more than 6 h. The ground PSS/DVB resin was added in the solution
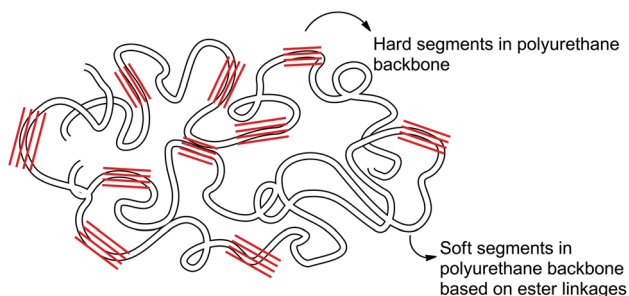

Fig. 1 Schematics of molecular structure of TPU consisting of hard and soft segments.

and stirring continued for another 3 h. The mixture was cast at a thickness of 120–130 μm using a film applicator (Sheen®, UK) on a clean glass plate at 25 °C. The TPU-PSS/DVB membranes adhered to the glass plate were air dried at 25 °C for 2 h and peeled off by soaking in distilled water. Table 1 enlists the compositions of TPU-PSS/DVB membranes based on varying PSS/DVB resin content.

2.4 Membrane structural and thermal analyses

The microscopic images of gold sputtered membrane specimens were obtained by scanning electron microscope (SEM, Hitachi S-300H). Fourier Transform Infrared Spectra (FTIR) of dry membrane specimens were obtained using JASCO® FTIR 4100 spectrophotometer in attenuated total reflectance (ATR) mode in wavenumber range 600–4000 cm^{-1}. Thermal degradation behaviour was studied using Schimadzu® TGA-50 under nitrogen environment in temperature range room temperature to 600 °C at 20 °C min^{-1} scan rate.

2.5 Water uptake measurement

Water uptake has significant effect on membrane's electrochemical properties. To measure water uptake, the membrane specimens of about 3 cm^2 were soaked in distilled water for 24 h. The excess surface water was wiped off with the aid of filter paper and membranes were weighed. The weight of the same membrane pieces was recorded once dried to the constant weight at 30 °C for 24 h. The water uptake was calculated by difference in the weight of the wet (W_{wet}) and dry (W_{dry}) membrane specimens as given by the following equation.[3,26–28]

$$\text{Water uptake(WU)} = \frac{W_{wet} - W_{dry}}{W_{dry}} \times 100 \qquad (1)$$

2.6 Ion exchange capacity

Ion exchange capacity (IEC) of membrane specimens was measured by titration method. Membrane specimens were immersed in 1 M hydrochloric acid for 24 h and washed with distilled water to remove any H$^+$ ions accumulated at the surface. The specimens were then equilibrated in 2 M sodium chloride (aqueous) for 24 h and titrated with 0.01 M sodium hydroxide (aqueous). The IEC is given by the following equation.[12,29]

$$\text{Ion exchange capacity(IEC)} = \frac{V_{NaOH} \times C_{NaOH}}{W_{dry}} \times 100 \qquad (2)$$

Where V_{NaOH}, C_{NaOH} and W_{dry} are the volume and concentration of NaOH solution used and weight of the dry membrane, respectively.

2.7 Membrane potential measurement

Membrane potential was measured using Gamry® interface 1000 Potentiostat by placing the membrane in a two-compartment permeation cell. Membrane specimen of 3 cm^2 area was interposed between two halves of the glass permeation cell where one half cell was filled with 1 M NaCl and the concentration in the other half cell was varied (0.001–1 M NaCl). Platinum electrodes were used to measure the electrical potential in both half cells. Prior to the potential study, the membrane specimens were equilibrated in 0.001 M NaCl for >24 h. The transport number for each membrane specimen was calculated using Nernst equation given below.[30]

$$V_{\text{Measured}} = \left(2t_i^m - 1\right) \frac{RT}{F} \ln\left(\frac{a_1}{a_2}\right) \qquad (3)$$

Here t_i^m is the transport number of the counter ions in TPU-PSS/DVB membranes, R is gas law constant, T is temperature, F is Faraday constant and a_1 and a_2 represent activity coefficients of Na$^+$ ion in respective compartments.[31]

2.8 Electrodialysis experiments

Electrodialysis (ED) experiments were performed using an in-house built three-compartment glass cell (Fig. 2) employing TPU-PSS/DVB as cation exchange and AMI (7001) as anion exchange membranes. The electrodialysis cell comprised of anodic, cathode and middle feed compartments each had a volume of 12 ml. Platinum electrodes were used in anodic and cathode compartments for voltage application. The middle (feed) compartment was separated by interposing TPU-PSS/DVB cation and AMI-7001 anion exchange membranes (3 cm^2 cross section area), respectively. After each electrodialysis experiment, total dissolved solid content (mg l^{-1}) in the middle feed compartment was measured and used as a performance indicator of TPU-PSS/DVB cation exchange membrane. Brackish water feed (3000 mg l^{-1}) was prepared by dissolving NaCl in distilled water. At the start of each experiment, the anode and cathode compartments were filled with distilled water and the
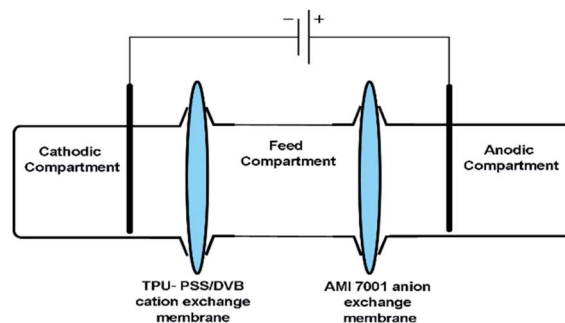
Table 1 Composition of various TPU-PSS/DVB ion exchange membranes

Sr. no.	TPU-PSS/DVB membranes	TPU binder : resin (%)
1	40 wt% PSS/DVB	60 : 40
2	50 wt% PSS/DVB	50 : 50
3	55 wt% PSS/DVB	45 : 55
4	60 wt% PSS/DVB	40 : 60

Fig. 2 Schematics of in-house built three-compartment electrodialysis cell.

middle compartment was filled with the feed. For these experiments, a constant DC source was used to apply potential difference of 7, 8 and 9 volt (V).[32] After each run, the concentration in the middle compartment was measured using HANNA TDS meter (Model HI8734). Salt extraction (SE) was calculated by the following equation,[33]

$$SE(\%) = \frac{C_i - C_f}{C_i} \times 100 \qquad (4)$$

where C_i and C_f represent initial and final salt concentrations of the middle (feed) compartment.

3. Results and discussion

3.1 SEM of TPU-PSS/DVB membranes

The SEM images of TPU-PSS/DVB membranes at varying PSS/DVB resin content are shown in Fig. 3. The cation exchange resin particles and TPU binder are clearly seen in these images as separate phases where the resin particles are uniformly distributed and completely embedded in TPU membrane matrix showing a strong interfacial adhesion between functional urethane moieties and $-SO_3^-$ groups of the cation exchange resin (Fig. 4b). The resin particles show a wide size distribution and some degree of agglomeration when the resin content increases in the membranes. On increasing the resin content beyond 50 wt%, the particles formed clusters that led to a continuous thread-like resin phase within the membrane (Fig. 3c and d). This might have resulted from the strong inter-particle adhesion of swollen resin particles and unique combination of hard and soft segments in the base TPU matrix. While soaked with water, these thread-like resin clusters swelled and developed physical flow channels that loosened membrane structure. Up to 50 wt% PSS/DVB resin content, the

electrochemical performance of the membranes is expected to be controlled by heterogeneous membrane morphology with a good resin distribution within TPU matrix. With further increase in resin content (55 and 60 wt%), the membrane started losing its electrochemical properties because of less compact morphology and excessive swelling in an electrolyte that resulted in semi-gelled phase morphology throughout membrane bulk. Thus, the membrane morphology associated with resin loading and distribution plays an important role in the membrane's electrochemical performance. Beyond 60 wt% resin content, the membrane lost its mechanical integrity completely and formed a distorted and broken gel phase in the electrolyte.

3.2 Water uptake and ion exchange capacity

Water uptake and ion exchange capacity (IEC) values of TPU-PSS/DVB membranes are given in Table 2. Increasing PSS/DVB resin content in the membrane increased water uptake from 45 to 63% and IEC value from 1.08 to 1.43 meq. g^{-1}. This might have resulted by introducing more functional groups into membrane phase ($-SO_3^-$ in this case) per unit volume that became hydrated by electrolyte and resulted in membrane swelling.

This high swelling behaviour may also be associated with the unique morphology of these TPU-PSS/DVB ion exchange membranes that resulted from strong hydrogen bonding between urethane–water and ester–water in addition to urethane–urethane and urethane–ester moieties in backbone chains (Fig. 4a). This hydrogen bonding facilitated the excessive swelling that increased water uptake to significantly higher values when compared to other heterogeneous membranes systems as shown in Table 3.[34] This water plasticization effect
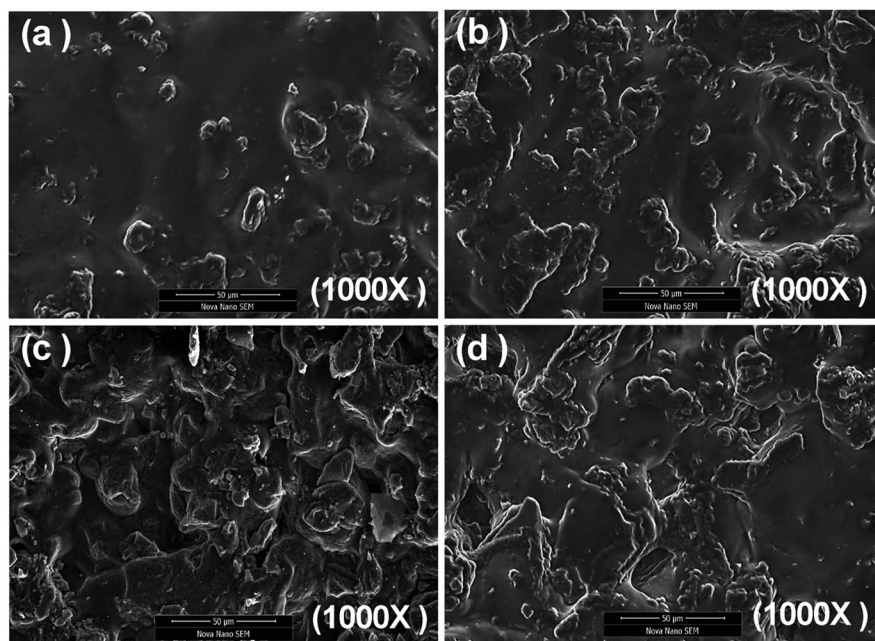

Fig. 3   SEM images (a–d) of 40, 50, 55 and 60 wt% PSS/DVB content respectively in TPU matrix membranes.
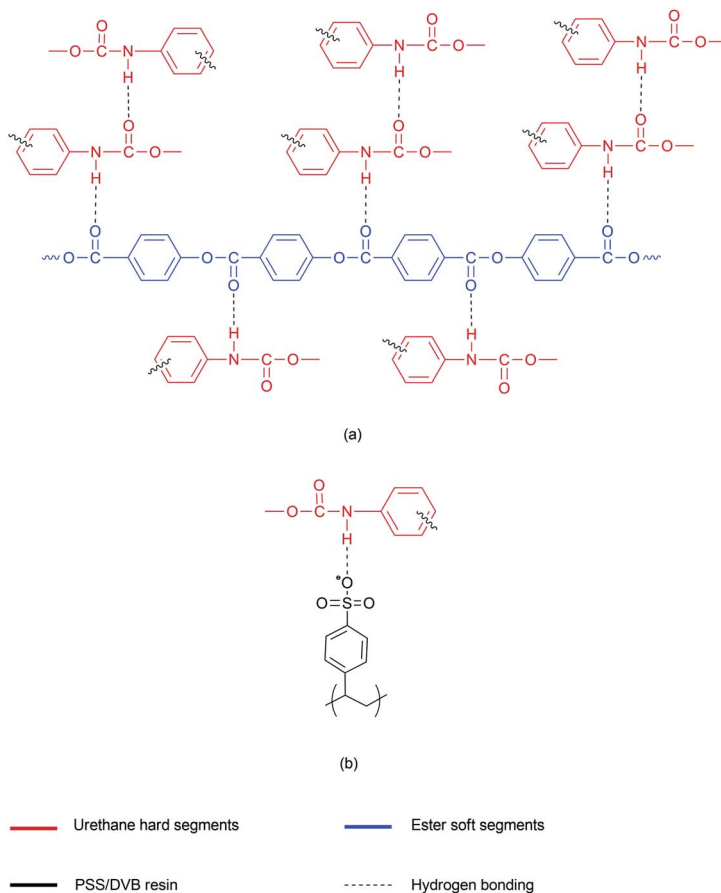
Fig. 4   Illustration of (a) urethane–urethane and urethane–ester hydrogen bonding (b) urethane–PSS/DVB hydrogen bonding in TPU-PSS/DVB membranes.

results from the interaction of TPU with water as already discussed resulted in highly swollen membrane morphology.[25] Hydrophilic polymers such as TPU with physical cross-links are capable to form polymer gels upon absorption of moisture in the cross-linked regions whereas this structure is thermally reversible.[35] These gels form soft structures with large amount of moisture residing in the polymer phase.

Initially, at lower resin content, the two-phase morphology in TPU-PSS/DVB membrane comprising a partially homogeneous gel phase of PSS/DVB resin and swollen hydrophilic TPU binder showed a compact morphology without forming voids and water channels (Fig. 3a and b) thus increasing the exposed functional sites of resin particles.[36] The hard segments in TPU owing to their higher mechanical properties provided adequate strength to the membrane to maintain two-phase semi-gelled morphology without developing additional water flow channels and pathways.[37,38] This partially homogeneous TPU-PSS/DVB gel structure retained compactness up to 50 wt% resin loading and beyond this (i.e. 55 and 60 wt%), the ratio of the hard segments to swollen PSS/DVB decreased, and the membrane structure turned less compact thus developing water flow channels and physical pathways (Fig. 3c and d). Dolmaire et al.[14] discussed the effects of the ratio of hydrophilic polyoxymethylene moieties in TPU and crosslinking/blending it with hydrophobic polydimethylsiloxane (PDMS). Balancing the hydrophilic/hydrophobic content in composite films and adjusting the crosslinking ratio in addition to the physical crosslinking originating from the hard segments of TPU

Table 2   Water uptake and ion exchange capacity values of TPU-PSS/DVB ion exchange membranes

Sr. no.	TPU-PSS/DVB membranes	Ion exchange capacity (meq. g^{-1})	Water uptake (%)
1	Pristine TPU	—	27
2	40 wt% PSS/DVB	1.08	45
3	50 wt% PSS/DVB	1.2	51
4	55 wt% PSS/DVB	1.32	54
5	60 wt% PSS/DVB	1.43	63

Table 3 Comparison of the properties of various ion exchange membranes with the present TPU-PSS/DVB membranes

Sr. no.	Name	Binder : resin/filler ratio	Type	t_i^m (Na$^+$)	IEC (meq. g^{-1})	Permselectivity	Water uptake (%)	Ref.
1	PC	40 : 60	Heterogeneous	0.91	1.8	0.86	27	40
2	PVC/ABS	50 : 50	Heterogeneous	0.77	1.6	0.65	25.8	41
3	SBR/PC	50 : 50	Heterogeneous	0.92	1.8	0.88	27.8	42
4	ABS/HIPS	50 : 50	Heterogeneous	0.88	1.5	0.80	29.5	43
5	PVC	30 : 70	Heterogeneous	0.92	3.0	—	—	10
6	PVC	50 : 50	Heterogeneous	0.90	—	0.84	18	44
7	S-PVC	40 : 60	Heterogeneous	0.90	1.9	0.84	40	40
8	CMI 7000	—	Heterogeneous	0.94	—	—	—	45
9	PVC–ZrAlP	25 : 75	Heterogeneous	0.89	—	0.82	10.3	47
10	CMF	—	Homogeneous	0.95	—	—	—	45
11	FKS	—	Homogeneous	0.96	—	—	—	45
12	SPEEK	—	Homogeneous	0.92	1.1	0.86	18.5	46
13	CMV (Asahi)	—	Homogeneous	—	2.4	0.95	25	39
14	HJC (Asahi)	—	Heterogeneous	—	1.8	—	51	39
15	CMX (Neosepta)	—	Heterogeneous	—	1.5–1.8	0.97	25–30	39
16	CMS (Neosepta)	—	Heterogeneous	—	2.0	—	38	39
17	Nafion 117 (DuPont)	—	Homogeneous	—	0.9	0.97	16	39
18	CMD	—	Homogeneous	0.94	—	—	—	45
19	FKB	—	Homogeneous	—	1.2	—	30	45
20	TPU-PSS/DVB	60 : 40	Heterogeneous	0.87	1.08	0.80	45	The present research
		50 : 50		0.95	1.2	0.92	51	
		45 : 55		0.89	1.3	0.82	54	
		40 : 60		0.84	1.4	0.73	63	

backbone chains, showed strong effects on water sorption and swelling extent. In the present work, the 50 wt% resin content in the membrane showed stable partially heterogeneous morphology and expected to show electrochemical performance controlled by resin content (Section 3.5 and 3.6) and above this content, the morphology shifted from a two-phase to a complete semi-gelled phase where the ionic leakages due to intrinsic water transport characteristics of hydrophilic TPU should influence the membrane performance. In a recent study of effects of incorporating bis(8-hydroxyquinoline)zinc (ZnQ_2) nanoparticles in PVC based heterogeneous ion exchange membrane revealed that increasing ZnQ_2 nanoparticles into membrane increased water uptake because of strong intermolecular interaction with water and beyond a certain extent (8%), the water uptake was maximum that led to wider ionic channels and loosen membrane structure thus decreasing selectivity.[3]

Although, the ion exchange capacity values of TPU-PSS/DVB membranes increased with resin content, but these do not follow the same trend as that of increase in water content (Table 2). For 5% increase of resin content from 50 to 55 wt% the water uptake increased from 51 to 54% but IEC increased from 1.2 to 1.32 only. A different trend was shown for 55 and 60 wt% resin content. This suggests that not only PSS/DVB content in the membrane but also their dissociation to $-SO_3^-$ moieties plays significant role in ion exchangeability that also depends on the water content in the membranes. A slight decline in increasing trend of IEC values at higher resin content suggests saturation in IEC on maximum water uptake. IEC values 1.2–1.4 meq. g^{-1} for TPU-PSS/DVB membranes are comparable to that of a number of commercial and research grade membranes as shown in Table 3 where a wide range of values are shown depending on polymer matrix type and resin/filler ratio.

3.3 Fourier transform infrared spectroscopy (FTIR)

The FTIR spectra of TPU-PSS/DVB membranes are shown in Fig. 5. The characteristics infrared bands for TPU are 3450 cm^{-1} representing NH stretch in the carbamate group, 2950 and 2970 cm^{-1} for C–H stretch, 1730 cm^{-1} for carbonyl stretch in polyester soft blocks in TPU backbone chain, 1533 cm^{-1} for

N–H bending, 1427 cm^{-1} is assigned to CH_2 stretch, 1539 cm^{-1} and 1310 cm^{-1} represent wagging of CH_3 and aromatic C–N bonds in carbamate, respectively, whereas the peaks at 1071–1281 cm^{-1} may be related to polyester (C–O) stretch.[15,48–50]

For PSS/DVB the characteristics IR peaks are 1600 cm^{-1} (aromatic C–C stretch), 1041 cm^{-1} (SO_3 symmetric vibration), 835 cm^{-1} (aromatic C–H vibration) and 756 cm^{-1} (out of plane bending of C–H in mono substituted benzene ring).[51]

The effect of PSS/DVB resin incorporation in the TPU membranes can also be shown in terms of strong hydrogen bonding and the resultant peak shift. The peak at 1730 cm^{-1} shifted to 1703 cm^{-1} in TPU-PSS/DVB membranes indicating the hydrogen bonded carbonyl stretch in the polyester soft block whereas the peak for polyester C–O stretch appeared at 1161 cm^{-1}.[34,50] The peak at 3337 cm^{-1} indicates the urethane–urethane straining due to hydrogen bonding.[52,53] Similarly, the peak at 822 cm^{-1} emerged probably because of the aromatic ring straining which can be explained by coupling with the peak 1041 cm^{-1} appeared at 1038 cm^{-1} that accounts for the stretching of $-SO_3$ groups because of the interaction with urethane groups. This interaction might have contributed to the decrease in charge density of negatively charged $-SO_3^-$ hence influencing the ion exchange capacity of membranes as discussed in Section 3.2. As the resin content increased in the membranes (40–60 wt%), the TPU characteristic peaks such as 3337, 1703, 1529, 1166 cm^{-1} decreased in intensity showing increasing PSS/DVB resin incorporation into TPU matrix.

3.4 Thermogravimetric analysis (TGA)

TGA thermograms of PSS/DVB resin and TPU-PSS/DVB membranes are shown in Fig. 6. The thermograms of PSS/DVB and TPU-PSS/DVB membranes showed a three-stage degradation behaviour. The higher mass loss in the TPU-PSS/DVB membranes as compared to PSS/DVB resin confirms a TPU dominant degradation behaviour in TPU-PSS/DVB membranes. For PSS/DVB, the first step shows dehydration up to 160 °C.[54] The subsequent weight loss shows desulfurization of PSS/DVB resin up to 380 °C. The third degradation step
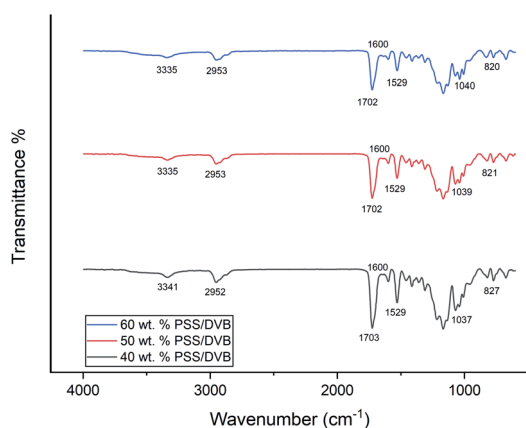

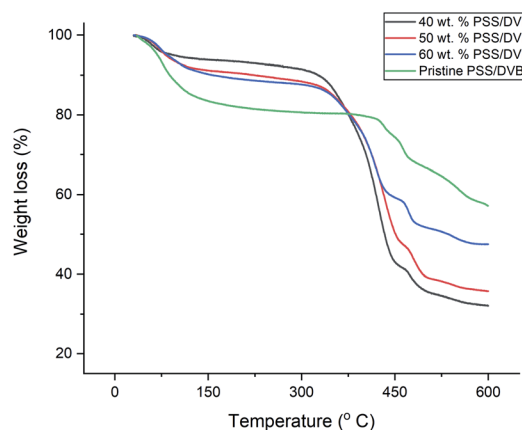**Fig. 5** FTIR-ATR spectra of TPU-PSS/DVB membranes.

Fig. 6 TGA thermograms of PSS/DVB resin and TPU-PSS/DVB membranes.

shown at 400–540 °C accounts for fusion and charring behaviour of PSS/DVB with minor emission of gaseous content.[54]

In TPU-PSS/DVB membranes, initial weight loss up to 160 °C can be attributed to residual moisture and solvent (MEK) loss in the membranes. The onset of TPU degradation is evident at around 370 °C involving degradation of hard segment in the form of disassociation of urethane into polyol and isocyanate that continues up to 450 °C.[55] The third degradation step starting around 460 °C can be related to the degradation of soft segment involving breakage of bonds formed through polycondensation and polyol degradation that continues up to 600 °C.[16]

3.5 Membrane potential measurement

In a highly swollen ion exchange membrane in an electrolyte, the measured potential across the membrane phase in a two-compartment cell is given by the following equation,

$$V_{\text{Measured}} = V_{\text{Don1}} + V_{\text{Diff}} + V_{\text{Don2}} \qquad (5)$$

Here V_{Don1}, V_{Don2} are Donnan potentials and V_{Diff} is the diffusional potential that results from the diffusion of ions across membrane phase. In higher concentrations of electrolyte, the Donnan potentials can be neglected and only diffusional potential represents ionic mobility across the membrane phase.[45] In this case, the measured potential across the membrane is related to the transport number of counter ions through Nernst equation as given below.[5,45]

$$V_{\text{Diff}} = \left(2t_i^m - 1\right)\left(\frac{RT}{F}\right)\ln\left(\frac{a_1}{a_2}\right) \qquad (6)$$

For similar electrolytes at both sides of the permeation cell (NaCl in the present case), the electroneutrality condition holds *i.e.* $t_{\text{Na}^+} + t_{\text{Cl}^-} = 1$. For approximation, the ratio of activity coefficients (a_1/a_2) can be replaced by ratio (C_1/C_2) *i.e.* with the concentration ratio.[56] The plots of V_{Diff} *vs.* $\ln(C_1/C_2)$ for various TPU-PSS/DVB membranes are shown in Fig. 7. The slope of diffusional potential V_{Diff} *vs.* $\ln(C_1/C_2)$ yields transport number of Na$^+$ counterions as given by eqn (6).[5] The ionic permselectivity (P_s) of these membranes for counter ions was calculated by the equation given below.[40,57,58]

$$P_s = \frac{t_i^m - t_o}{t_o} \qquad (7)$$

Where t_o is the transport number of counter ion in the solution and t_i^m is the transport number of the counter ion calculated using Nernst equation (eqn (6)) in the membrane phase.[40]

For PSS/DVB resin increment from 40 to 50 wt%, the membrane potential increased from 0.13 to 0.15 V. This rise can be attributed to increased concentration of PSS/DVB charge moieties in membrane matrix. For 50 wt% PSS/DVB resin content, the uniform distribution of PSS/DVB resin and development of conducting regions for counter ions improved electrochemical properties whereas the membrane did not show any voids or physical pathways for water flow. The highest transport number (*i.e.*, 0.95) was recorded for 50 wt% PSS/DVB
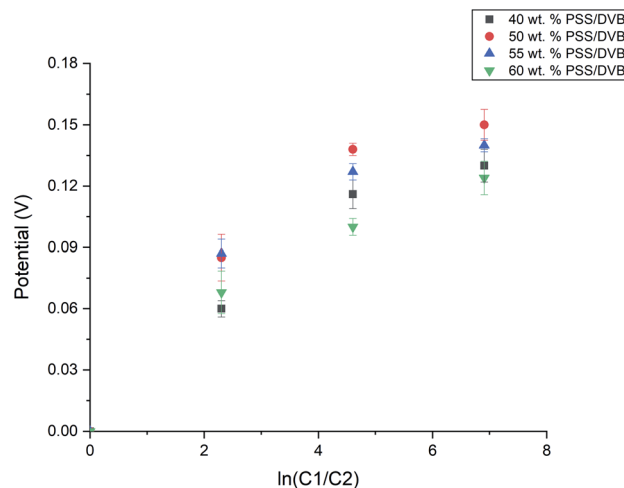
Fig. 7 Membrane potentials of TPU-PSS/DVB membranes.

content. This can be related to the two-phase membrane morphology as discussed in Section 3.2. The membrane's semi-gelled morphology increased its electrochemical properties up to 50 wt% resin content whereas further increase in the resin content (55 and 60 wt%) decreased the electrochemical properties of membrane (Table 3). This decrease can be attributed to the excessive swelling and water uptake that reduced the mechanical properties of membrane. The strength of hard segments was weakened by excessive swelling and water uptake. This mechanical failure originated from the gel phase rupture led to the development of physical pathways and water flow channels that facilitated the transport of co-ions hence reducing the transport number (from 0.95 to 0.89 and 0.84) (Fig. 8). The highest values of transport number and permselectivity also suggested 50 wt% resin as an optimum content that is in line with the previously discussed IEC and membrane water uptake values. The effects of membrane morphology on lowering transport numbers and permselectivity have been discussed for PVC based heterogeneous
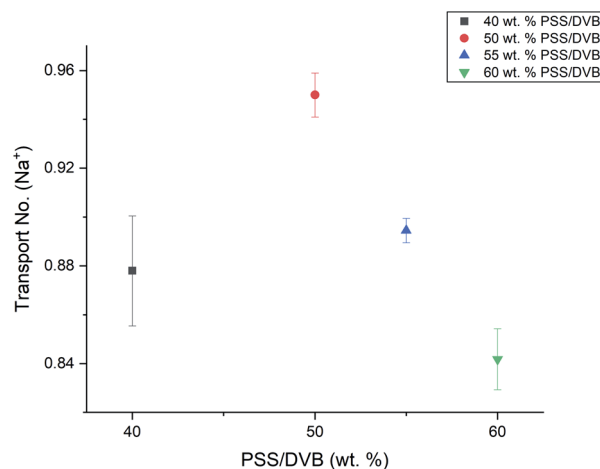
Fig. 8 Transport number of TPU-PSS/DVB membranes.

membrane.[3] In that study, the incorporation of ZnQ_2 nanoparticles increased membrane swelling and beyond a threshold value, it loosened the membrane structure resulted in excessive swelling that introduced co-ion leakage thus decreased transport numbers and permselectivity.

Comparing IEC, transport numbers and water uptake values of TPU-PSS/DVB membranes with the previously published literature (Table 3), it can be inferred that the ion exchange membranes showed a wide variation in these electrochemical parameters depending on composition and morphology. A generalized trend of lower water uptake and transport numbers with higher IEC values can be seen for heterogeneous membranes. A few of homogeneous membranes showed higher water uptake with high perm-selectivity values (i.e., sulfonated polyether-ether ketone (SPEEK) membranes). The TPU-PSS/DVB membranes in the present study showed higher water uptake (51%) with higher perm-selectivity (0.92) at 50 wt% resin content that suggests a two-phase morphology in TPU-PSS/DVB membranes with a PSS/DVB semi-gelled phase. At higher resin loading (i.e., >50 wt%), the swelling throughout the membrane bulk dominates the permeation behaviour with ionic leakage thus decreasing both transport numbers and permselectivity.

3.6 Electrodialysis study

The electrodialytic salt extraction study of TPU-PSS/DVB membranes was conducted with varying resin content (i.e., 40, 50, 55 and 60 wt% PSS/DVB). Table 4 shows salt extraction values (%) of feed (initially 3000 mg l^{-1} NaCl) for 1 h electrodialysis using an in-house built three-compartment electrodialysis cell at varying voltage (7–9 V). The membranes with 40 and 50 wt% PSS/DVB contents showed increased salt extraction (from 16 to 20 and 27%, respectively) with increasing voltages (7, 8 and 9 V). These membranes had higher transport numbers and compact membrane morphology without water flow channels that resulted in increasing electrodialytic salt extraction with increasing voltage. In contrary, the membranes with higher resin content (55 and 60 wt% PSS/DVB) showed a continuous decrease in salt extraction with increasing voltage (i.e. from 19 to 15 and 17 to 13%). As discussed in Section 3.5, these membranes developed water flow channels and physical pathways for both counter and co-ions because of excessive swelling by overcoming physical crosslinking and the mechanical strength of hard segments of TPU backbone chains. This swelling led to a semi-gelled membrane structure

throughout the bulk. Salt extraction (SE, %) have been used previously to assess the ED efficiency of both the IEMs and ED cells in three-compartment and multi-stack electrodialysis set up.[25,59–65] Amado et al.[25] used a three-compartment electrodialysis setup by employing a number of membranes deposited with electroactive polyaniline (PANI) and reported salt extraction values ranging from 17 to 30%. Wang et al.[62] used a modified three-compartment electrodialytic cell with varying voltage (15–40 V) and flow rates (15–40 l h^{-1}) and showed SE values around 69%. Kirkelund et al.[63] presented a comparison of two- and three-compartment electrodialytic separation of heavy metals from contaminated water resources. A range of SE values was reported (10–91%) depending on the nature of contaminated water resource. Zhao et al.[64] modified cation exchange membranes with electroactive polyaniline (PANI) and measured various properties (i.e., IEC = 0.47, WU = 48%, t_{Na}^+ = 0.93) and showed salt extraction ranging from 5 to 86% in 20 min to 6 h electrodialysis experiments. Abdel-Aal et al.[65] used a multi-stack electrodialysis setup for desalination of high salinity water with increasing voltage (6 to 18 V for 30 min) and showed separation efficiency upto 94.8%. This study correlated SE values with applied voltage across membranes stack/cell, membrane area and number of membrane stacks (pairs). A number of other researchers have also shown a wide variation in membranes characteristics and electrodialysis performance of their membranes at varying operational conditions. The operational variables in electrodialysis such as feed flow rate, number of membrane pairs (i.e., stack of cation–anion exchange membranes) and membrane working area have pronounced effects on electrodialysis performance i.e. salt extraction (%) in addition to membrane characteristics such as chemical nature (functionality) IEC, swellability and transport numbers.[60] The optimum flow rate is essential for effective desalination as increasing flow rate increases desalination rate by decreasing the thickness of diffusional boundary layer. Moreover, the higher number of membrane pairs and continuous recirculation of the feed at optimum flow rate may improve the effective contact of feed water with membranes thus resulting in more efficient desalination.[65–69]

4. Conclusion

Novel heterogeneous cation exchange membranes based on partially hydrophilic polyester based thermoplastic polyurethane incorporated with PSS/DVB cation exchange resin were prepared through solution casting technique and characterized for various properties. The effects of resin incorporation level in the membranes have been studied in a systematic way. The FTIR spectra of TPU-PSS/DVB membranes suggested hydrogen bonding interactions of water with TPU molecular chains and physical crosslinking between the hard segments of TPU that resulted in excessive water uptake. The transport numbers, permselectivity and salt extraction increased by increasing PSS/DVB resin content up to 50 wt% along with membrane water uptake and ion exchange capacity (IEC). Based on SEM micrographs, a two-phase membrane morphology was suggested comprising hard and soft segmented TPU backbone

Table 4 Electrodialytic salt extraction (%) for TPU-PSS/DVB membranes

Salt extraction of TPU-PSS/DVB membranes (SE, %)

Sr. no.	Voltage	40 wt% PSS/DVB	50 wt% PSS/DVB	55 wt% PSS/DVB	60 wt% PSS/DVB
1	7	16	20	19	17
2	8	19	24	18	14
3	9	20	27	15	13

matrix and uniformly distributed PSS/DVB resin particles. FTIR spectra indicated hydrogen bonding among urethane, $-SO_3^-$ and water moieties. On increasing the resin content beyond 50 wt%, the excessive swelling developed a semi-gelled phase throughout membrane bulk with the introduction of voids and flow channels. Therefore, the transport numbers, salt extraction and permselectivity decreased whereas water uptake and IEC values increased. This highlights the need of optimum resin loading in a heterogeneous ion exchange membrane system keeping in view the structural characteristics of matrix polymer. The swollen membrane morphology greatly influenced the transport number of the membrane because of the co-ion leakage on swelling. Comparing with various commercial and research grade membranes, the present study showed a successful development of heterogonous cation exchange membrane based on TPU with acceptable electrodialytic performance.

Conflicts of interest

There are no conflicts to declare.

Acknowledgements

References

1 S. H. Shin, Y. Kim and S. H. Moon, *RSC Adv.*, 2015, **5**, 37206.
2 M. Y. Kariduraganavar, R. K. Nagarale, A. A. Kittur and S. S. Kulkarni, *Desalination*, 2006, **197**, 225.
3 S. M. Hosseini, E. Jashni, M. R. Jafari, B. Van der Bruggen and Z. Shahedi, *J. Membr. Sci.*, 2018, **560**, 1.
4 S. M. Hosseini, S. Sohrabnejad, G. Nabiyouni, E. Jashni, B. Van der Bruggen and A. Ahmadi, *J. Membr. Sci.*, 2019, **583**, 292.
5 M. S. Malik, A. A. Qaiser and M. A. Arif, *RSC Adv.*, 2016, **6**, 115046.
6 S. M. Hosseini, M. Askari, P. Koranian, S. S. Madaeni and A. Moghadassi, *J. Ind. Eng. Chem.*, 2014, **20**, 2510.
7 P. V. Vyas, B. G. Shah, G. S. Trivedi, P. Ray, S. K. Adhikary and R. Rangarajan, *J. Membr. Sci.*, 2001, **187**, 39.
8 S. M. Hosseini, S. S. Madaeni, A. Zendehnam, A. R. Moghadassi, A. R. Khodabakhshi and H. Sanaeepur, *J. Ind. Eng. Chem.*, 2013, **19**, 854.
9 D. Ariono, Khoiruddin, D. Prabandari, R. Wulandari and I. G. Wenten, *J. Phys.: Conf. Ser.*, 2017, **877**, 012075.
10 P. V. Vyas, B. G. Shah, G. S. Trivedi, P. Ray, S. K. Adhikary and R. Rangarajan, *React. Funct. Polym.*, 2000, **44**, 101.
11 A. Moghadassi, P. Koranian, S. M. Hosseini, M. Askari and S. S. Madaeni, *J. Ind. Eng. Chem.*, 2014, **20**, 2710.
12 S. M. Hosseini, B. Rahzani, H. Asiani, A. R. Khodabakhshi, A. R. Hamidi, S. S. Madaeni, A. R. Moghadassi and A. Seidypoor, *Desalination*, 2014, **345**, 13.
13 Z. Maghsoud, M. Pakbaz, M. H. N. Famili and S. S. Madaeni, *J. Membr. Sci.*, 2017, **541**, 271.
14 N. Dolmaire, F. Méchin and E. Espuche, *Desalination*, 2006, **199**, 118.
15 T. Wu and B. Chen, *Sci. Rep.*, 2017, **7**, 1.
16 S. Anandhan and H. Lee, *J. Elastomers Plast.*, 2012, **46**, 217.
17 M. M. Talakesh, M. Sadeghi, M. P. Chenar and A. Khosravi, *J. Membr. Sci.*, 2012, **415–416**, 469.
18 T. Jiříček, M. Komárek and T. Lederer, *J. Nanotechnol.*, 2017, **2017**, 1.
19 M. Sadeghi, M. M. Talakesh, B. Ghalei and M. Shafiei, *J. Membr. Sci.*, 2013, **427**, 21.
20 M. B. Karimi, G. Khanbabaei and G. M. M. Sadeghi, *J. Membr. Sci.*, 2017, **527**, 198.
21 Q. Meng, J. Hu and S. Mondal, *J. Membr. Sci.*, 2008, **319**, 102.
22 S. Nazemidashtarjandi, S. A. Mousavi and D. Bastani, *Journal of Water Process Engineering*, 2017, **16**, 170.
23 M. Zhang, B. Liao, X. Zhou, Y. He, H. Hong, H. Lin and J. Chen, *Bioresour. Technol.*, 2015, **175**, 59.
24 H. Júnior, D. Bertuol, Á. Meneguzzi, C. A. Ferreira and F. Amado, *Mater. Res.*, 2013, **16**, 860.
25 F. D. R. Amado, L. F. Rodrigues, M. A. S. Rodrigues, A. M. Bernardes, J. Z. Ferreira and C. A. Ferreira, *Desalination*, 2005, **186**, 199.
26 M. Mokhtar, S. E. Dickson, Y. Kim and W. Mekky, *J. Ind. Eng. Chem.*, 2018, **60**, 475.
27 H. Lee, J. Han, K. Kim, J. Kim, E. Kim, H. Shin and J. C. Lee, *J. Ind. Eng. Chem.*, 2019, **74**, 223.
28 H. Farrokhzad, T. Kikhavani, F. Monnaie, S. N. Ashrafizadeh, G. Koeckelberghs, T. Van Gerven and B. Van der Bruggen, *J. Membr. Sci.*, 2015, **474**, 167.
29 H. Farrokhzad, S. Darvishmanesh, G. Genduso, T. Van Gerven and B. Van Der Bruggen, *Electrochim. Acta*, 2015, **158**, 64.
30 S. M. Hosseini, Z. Ahmadi, M. Nemati, F. Parvizian and S. S. Madaeni, *Water Sci. Technol.*, 2016, **73**, 2074.
31 A. A. Qaiser, M. M. Hyland and D. A. Patterson, *J. Membr. Sci.*, 2011, **385–386**, 67.
32 M. Sadrzadeh and T. Mohammadi, *Desalination*, 2008, **221**, 440.
33 L. J. Banasiak, T. W. Kruttschnitt and A. I. Schäfer, *Desalination*, 2007, **205**, 38.
34 F. S. Yen, L. L. Lin and J. L. Hong, *Macromolecules*, 1999, **32**, 3068.
35 J. E. H. Sánchez, K. Müller and W. Possart, *Int. J. Adhes. Adhes.*, 2016, **66**, 167.
36 D. Ariono, K. Khoiruddin, S. Subagjo and I. G. Wenten, *Mater. Res. Express*, 2017, **4**, 024006.
37 S. Oprea, *High Perform. Polym.*, 2005, **17**, 163.
38 Y. Guo, R. Zhang, Q. Xiao, H. Guo, Z. Wang, X. Li, J. Chen and J. Zhu, *Polymer*, 2018, **138**, 242.
39 R. K. Nagarale, G. S. Gohil and V. K. Shahi, *Adv. Colloid Interface Sci.*, 2006, **119**, 97.
40 S. M. Hosseini, S. S. Madaeni and A. R. Khodabakhshi, *Sep. Sci. Technol.*, 2011, **46**, 794.
41 M. Namdari, T. Kikhavani and S. N. Ashrafizadeh, *Ionics*, 2017, **23**, 1745.

42 S. M. Hosseini, S. S. Madaeni and A. Reza, *J. Membr. Sci.*, 2010, **362**, 550.

43 S. M. Hosseini, S. S. Madaeni and A. Reza, *J. Membr. Sci.*, 2010, **351**, 178.

44 S. M. Hosseini, S. Rafiei, A. R. Hamidi, A. Moghadassi and S. S. Madaeni, *Desalination*, 2014, **351**, 138.

45 Y. Tanaka, *Ion Exchange Membranes Fundamentals and Applications*, Elsevier B.V., Amsterdam, 2nd edn, 2015.

46 D. T. Chakrabarty, M. Kumar, K. P. Rajesh, V. Shahi and N. Srinivasan, *Sep. Purif. Technol.*, 2010, **75**, 174.

47 S. Imteyaz and Rafiuddin, *RSC Adv.*, 2015, **5**, 96008.

48 S. Todros, C. Venturato, A. N. Natali, G. Pace and V. Di Noto, *J. Polym. Sci., Part B: Polym. Phys.*, 2014, **52**, 1337.

49 L. Ning, W. De-Ning and Y. Sheng-Kang, *Macromolecules*, 1997, **30**, 4405.

50 M. Kathalewar, N. Dhopatkar, B. Pacharane, A. Sabnis, P. Raut and V. Bhave, *Prog. Org. Coat.*, 2013, **76**, 147.

51 S. B. Brijmohan, S. Swier, R. A. Weiss and M. T. Shaw, *Ind. Eng. Chem.*, 2005, **44**, 8039.

52 L. Karimi, A. Ghassemi and H. Zamani Sabzi, *Desalination*, 2018, **445**, 159.

53 T. Qiang, I. Krakovský, G. Yan, L. Bai, J. Liu, G. Sun, L. Rosta, B. Chen and L. Almásy, *Polymers*, 2016, **8**, 197.

54 R. Scherer, A. M. Bernardes, M. M. C. Forte, J. Z. Ferreira and C. A. Ferreira, *Mater. Chem. Phys.*, 2001, **71**, 131.

55 M. Kannan, S. S. Bhagawan, S. Thomas and K. Joseph, *J. Therm. Anal. Calorim.*, 2012, **112**, 1231.

56 B. Bei Wang, M. Wang, K. Kai Wang and Y. Xiang Jia, *Desalination*, 2016, **384**, 43.

57 S. M. Hosseini, M. Nemati, F. Jeddi, E. Salehi, A. R. Khodabakhshi and S. S. Madaeni, *Desalination*, 2015, **359**, 167.

58 T. Sata, *Ion exchange membranes: Preparation, Characterization, Modification and Application*, RSC, Cambridge, 2004.

59 T. Benvenuto, M. Antonio, S. Rodrigues and J. Zoppas-ferreira, *J. Cleaner Prod.*, 2017, **155**, 130.

60 D. G. Hassell, I. H. Dakhil and H. A. Hasan, *Chem. Eng. J.*, 2019, 122231.

61 A. Merkel, A. M. Ashra and M. Ondru, *Journal of Water Process Engineering*, 2017, **20**, 123.

62 D. Wang, X. Gao, Y. Zhang, L. Mao, Z. Wang and C. Gao, *Sep. Purif. Technol.*, 2017, **186**, 135.

63 G. M. Kirkelund, P. E. Jensen, L. M. Ottosen and K. B. Pedersen, *J. Hazard. Mater.*, 2019, 68.

64 J. Zhao, L. Sun, Q. Chen, H. Lu and J. Wang, *J. Membr. Sci.*, 2019, **582**, 211.

65 E. A. Abdel-Aal, M. E. Farid, F. S. M. Hassan and A. E. Mohamed, *Egypt. J. Pet.*, 2015, **24**, 71.

66 S. Gmar, N. Helali, A. Boubakri, I. Ben and S. Sayadi, *Appl. Water Sci.*, 2017, **7**, 4563.

67 H. Yan, Y. Wang, L. Wu, M. A. Shehzad, C. Jiang, R. Fu, Z. Liu and T. Xu, *J. Membr. Sci.*, 2019, **570–571**, 245.

68 O. Kedem, *J. Membr. Sci.*, 2002, **206**, 333.

69 L. J. Banasiak, T. W. Kruttschnitt and A. I. Schäfer, *Desalination*, 2007, **205**, 38.